# RADIATION PRESSURE ON PLASMA TURBULENCE BY RADIO FREQUENCY WAVES

A.K. Ram
Plasma Science and Fusion Center, Massachusetts Institute of Technology
Cambridge MA, USA
Email: abhay@mit.edu

K. Hizanidis
National Technical University of Athens
157 73 Zographou, Greece

**Abstract**

The use of radio frequency (RF) waves in fusion devices – primarily, to modify and control the heating and current profiles, and to subdue deleterious instabilities – has been gaining traction over the last few decades. The antennas or waveguide structures used for launching electromagnetic waves are usually located in the vicinity of the outer wall of a device. Consequently, for coupling RF power to core plasma, the waves have to propagate through a turbulent scrape-off layer plasma in the edge region. The RF waves can scatter off the turbulence, thereby altering the power profile coupled to the core. Simultaneously, the radiation pressure of the RF waves can affect the turbulence. Theoretically, it is convenient to analyze the two effects separately and explore the underlying physics. There have been a number of analytical and computational studies on the scattering of RF waves by different forms of plasma turbulence. This paper explores the impact of radiation pressure on turbulence.

## 1. INTRODUCTION

A wide variety of density fluctuations are ubiquitous in magnetically confined fusion devices. In the scrape-off layer, fluctuations are a mix of incoherent turbulence and coherent structures commonly referred to as filaments or blobs [1], while fluctuations in the core plasma are induced by various instabilities. Radio frequency (RF) electromagnetic waves, commonly used for heating and for generating plasma currents, interact with the scrape-off layer fluctuations as they propagate from an antenna into the plasma. Analytical and computational studies show that turbulence modifies RF wave characteristics through reflection, refraction, side-scattering, diffraction, and shadowing [2-7]. This scattering has an undesirable effect on the efficiency of heating and current drive. However, the RF waves can also affect turbulence through radiation pressure [8]. This pressure is significant if there is a narrow transition layer – in effect, an interface – separating two different density regions. For electron cyclotron waves, the radiation pressure changes the density profile inside the scrape-off layer and can lead to peaking of the density profile in the core plasma. The latter effect has been observed in recent experiments [9]. For moderate RF power, the radiation force induces local acceleration of the plasma which ranges from tens to hundreds of meters per square second [8].

In this paper, we will discuss two approaches to studying radiation pressure by RF waves. The first approach applies to wave-like turbulence that can occur in the scrape-off layer and in the core plasma. The second approach will deal with the radiation pressure exerted on cylindrical filamentary structures that are common in the edge region of a fusion device.

In 1905, Poynting reported his theoretical and experimental research on the radiation pressure exerted on a planar interface separating two different dielectrics [10]. By imposing conservation of momentum, Poynting asserted that the pressure exerted on a vacuum-glass interface by ordinary light always points towards the vacuum – independent of whether the light is incident on the interface from the vacuum or from within the glass. We use the Kirchhoff tangent plane approximation [11,12] to determine the radiation pressure on a turbulent layer separating two different plasma densities. We show that, in accordance with Poynting's results, the RF waves tend to push an interface separating two different plasma densities towards the region of higher density. Unlike ordinary dielectrics in which the opacity increases with increasing density, a plasma has the opposite property. Its refractive index is less than that of vacuum and decreases with increasing electron density. Thus, the higher density plasma has a lower refractive index than a lower density plasma. Consequently, the radiation pressure pushing the interface towards higher electron densities is equivalent to the pressure pushing it towards lower index of refraction. This is consistent with Poynting's conclusion for ordinary dielectrics where the interface is being

pushed towards the region of lower refractive index. The agreement between ordinary dielectrics and a plasma is not obvious at first glance. The propagation of waves in a magnetized plasma, represented by a tensor permittivity, is different from wave propagation in a scalar dielectric. In particular, for a given frequency, there are two waves with disparate wavelengths and polarizations that coexist in a cold plasma. For a particular choice of an incident wave, the scattering off density fluctuations couples power to the second wave [2,3]. However, this does not seem to affect the underlying physics of radiation pressure.

While the tangent plane approximation is applicable to plasma turbulence, it cannot be extended to scattering by density filaments. The spatial localization of a filament, as opposed to the infinite extent of a tangent plane, requires a different approach. The geometry plays an important role; a cylindrical filament leads to diffraction and shadowing – effects which do not appear in scattering by infinite planar surfaces. In the tangent plane approximation, the analysis relies on geometric optics. For a filament, we have to generalize to physical, full wave, optics [2,3]. Accordingly, we use the Maxwell stress tensor [13-15] to evaluate the radiation pressure on a cylindrical filament. We find that the direction of the pressure induced by RF waves does not necessarily follow Poynting's conclusion. The impact of the radiation pressure can be different; filaments with densities higher than the background density can be pulled towards the antenna [8].

## 2. MAXWELL EQUATIONS FOR A COLD PLASMA

We consider electromagnetic wave propagation in a cold magnetized plasma with no free charges and currents. The two Gauss equations for the electric displacement field and for the magnetic field can be treated as initial conditions. The Faraday and Ampere-Maxwell equations can be combined to yield,

$$\nabla \times \left( \nabla \times \mathbf{E}\left(\mathbf{r}\right) \right) - \frac{\omega^2}{c^2} \overline{\mathbb{K}}\left(\mathbf{r}\right) \cdot \mathbf{E}\left(\mathbf{r}\right) = 0, \tag{1}$$

where we have assumed that the time dependence of all fields is of the form $\exp\left(-i\omega t\right)$. Additionally, the cold plasma permittivity tensor $\overline{\mathbb{K}}$ is [15],

$$\overline{\mathbb{K}}\left(\mathbf{r}\right) = \begin{bmatrix} K_\perp & -iK_{xy} & 0 \\ iK_{xy} & K_\perp & 0 \\ 0 & 0 & K_\parallel \end{bmatrix}, \tag{2}$$

with,

$$\begin{aligned} K_\perp &= 1 - \frac{\omega_{pe}^2}{\omega^2 - \omega_{ce}^2} - \sum_i \frac{\omega_{pi}^2}{\omega^2 - \omega_{ci}^2}, \\ K_{xy} &= -\frac{\omega_{ce}}{\omega} \frac{\omega_{pe}^2}{\omega^2 - \omega_{ce}^2} + \sum_i \frac{\omega_{ci}}{\omega} \frac{\omega_{pi}^2}{\omega^2 - \omega_{ci}^2}, \\ K_\parallel &= 1 - \frac{\omega_{pe}^2}{\omega^2} - \sum_i \frac{\omega_{pi}^2}{\omega^2}, \end{aligned} \tag{3}$$

$\omega_{pe}$ ($\omega_{pi}$) and $\omega_{ce}$ ($\omega_{ci}$) are electron (ion) angular plasma and cyclotron frequencies, respectively, and the summation is over all ion species in the plasma. We have assumed that the plasma is embedded in a uniform magnetic field $\mathbf{B}_0 = B_0\hat{\mathbf{z}}$, where $\hat{\mathbf{z}}$ is a unit vector along the $z$-axis. For a plane wave with spatial dependence of the form $\exp\left(i\mathbf{k}\cdot\mathbf{r}\right)$, (1) reduces to an algebraic equation,

$$\overline{\mathbb{D}} \cdot \mathbf{E} = 0, \tag{4}$$

where $\mathbf{E}$ is a complex (vector) amplitude of the electric field and,

$$\overline{\mathbb{D}} = \frac{c^2}{\omega^2}\left(\mathbf{kk} - k^2\overline{\mathbb{I}}\right) + \overline{\mathbb{K}}. \tag{5}$$

In this equation $\mathbf{kk}$ is a dyadic and $\overline{\mathbb{I}}$ is the identity tensor of rank 2. For a non-trivial solution to $\mathbf{E}$, (4) requires that $\det\left(\overline{\mathbb{D}}\right) = 0$, where det denotes the determinant of the rank 2 tensor. This leads to the dispersion relation for electromagnetic waves in a plasma.

If we assume that the plasma density varies in the $x$ direction and is homogeneous in the $y$ direction, then $\mathbf{k} = k_\perp \hat{\mathbf{x}} + k_\parallel \hat{\mathbf{z}}$. The dispersion relation takes the form,

$$K_\perp n_\perp^4 + \left\{ K_{xy}^2 - \left(K_\perp + K_\parallel\right)\left(K_\perp - n_\parallel^2\right)\right\} n_\perp^2 + K_\parallel \left\{ \left(K_\perp - n_\parallel^2\right)^2 - K_{xy}^2 \right\} = 0, \tag{6}$$

where $n_\perp = ck_\perp/\omega$ and $n_\parallel = ck_\parallel/\omega$. For a given $n_\parallel$, there are two independent values of $n_\perp$ that satisfy (6). Thus, a cold plasma supports two plane wave eigenmodes which could be associated with propagating or evanescent waves.

## 3. KIRCHHOFF TANGENT PLANE APPROXIMATION

For the interaction of RF waves with incoherent fluctuations, the Kirchhoff tangent plane approximation is suitable for gaining physical insight into scattering and into the radiation pressure. The approximation is commonly used for modeling scattering of waves from rough surfaces [11,12]. As illustrated in Fig. 1, consider a surface $x = f(y,z)$ separating two spatial domains with different (homogeneous) electron densities $n_0$ and $n_1$. The tangent plane approximation is based on two assumptions. The first assumption is that, for an incident plane wave, the scattered fields are determined by the wave fields on the surface. The second assumption is that each point on the surface is part of an infinitely homogeneous plane that is tangent to this point. Subsequent to these assumptions, we make use of geometrical optics to determine the scattered fields and evaluate the local radiation pressure on the surface. This approach is similar to that used for deriving Snell's laws and the Fresnel equations for isotropic dielectrics [14]. In Fig. 1, the dashed line is tangent to one particular point $A(x_0, y_0, z_0)$ on the turbulent surface. It also represents an intersection of the tangent plane with the $x$-$z$ plane. A local normal to the tangent plane is given by,

$$\hat{\mathbf{n}} = \frac{\nabla\zeta}{||\nabla\zeta||}, \qquad \text{where } \zeta = \zeta(x,y,z) = x - f(z,y) = 0. \tag{7}$$

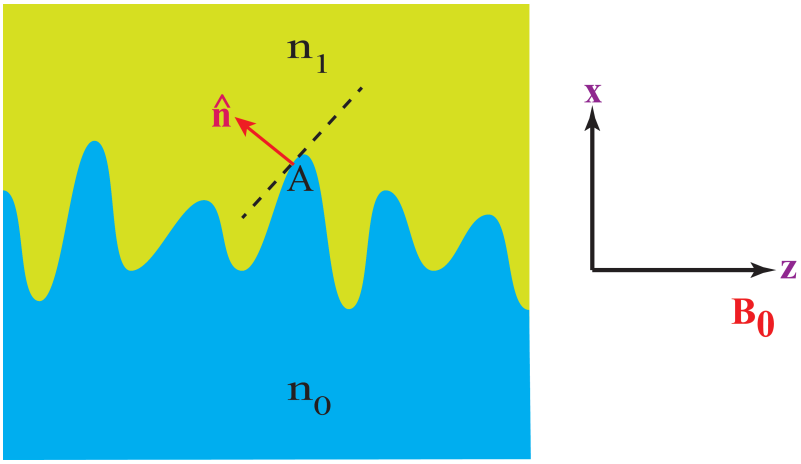


*FIG. 1. A representation of density fluctuation separating two different regions of electron density $n_0$ and $n_1$. The ambient magnetic field is along the $\hat{\mathbf{z}}$ direction, and the density varies along the $\hat{\mathbf{x}}$ direction. The dashed line is tangent to a point $A$ on this surface represented by the equation $x = f(y,z)$. The normal to the tangent plane is $\hat{\mathbf{n}}$. For a homogeneous plasma along $\hat{\mathbf{y}}$, $x = f(z)$.*

We choose a different Cartesian coordinate system defined by the unit vectors $(\hat{\mathbf{x}}', \hat{\mathbf{y}}', \hat{\mathbf{z}}')$, where $\hat{\mathbf{n}} = \hat{\mathbf{x}}'$, and the tangent plane lies in the $\hat{\mathbf{y}}'$-$\hat{\mathbf{z}}'$ plane. The mapping of $(\hat{\mathbf{x}}', \hat{\mathbf{y}}', \hat{\mathbf{z}}')$ into $(\hat{\mathbf{x}}, \hat{\mathbf{y}}, \hat{\mathbf{z}})$ is achieved through two Euler rotations given by angles $\theta$ and $\phi$,

$$\begin{bmatrix} \hat{\mathbf{x}}' \\ \hat{\mathbf{y}}' \\ \hat{\mathbf{z}}' \end{bmatrix} = \begin{bmatrix} \cos\theta & \sin\theta & 0 \\ -\sin\theta & \cos\theta & 0 \\ 0 & 0 & 1 \end{bmatrix} \begin{bmatrix} \cos\phi & 0 & -\sin\phi \\ 0 & 1 & 0 \\ \sin\phi & 0 & \cos\phi \end{bmatrix} \begin{bmatrix} \hat{\mathbf{x}} \\ \hat{\mathbf{y}} \\ \hat{\mathbf{z}} \end{bmatrix}. \tag{8}$$

At the point A in Fig. 1, the Euler angles are given by,

$$\tan\phi = -\frac{z_0}{x_0}, \qquad \tan\theta = \frac{y_0}{x_0\cos\phi - z_0\sin\phi}. \tag{9}$$

For a plasma that is homogeneous in the $y$ direction, the tangent planes will lie in the $x$-$z$ plane. One representation of a tangent plane is given in Fig. 2 where the interface between the two different electron densities is inclined at an angle $\phi$ with respect to the $z$ axis. The two regions with different electron densities are equivalent to two regions with different dielectric permittivities. Just as in the conventional derivation of the Fresnel equations and Snell's law in scalar dielectrics [14], a plane wave incident on this interface will be partially reflected and partially transmitted. However, in contrast to ordinary dielectrics, there will be two different reflected waves and two different transmitted waves in a plasma. This is a consequence of (6) – a cold plasma supports two different normal modes of propagation (or, evanescence).

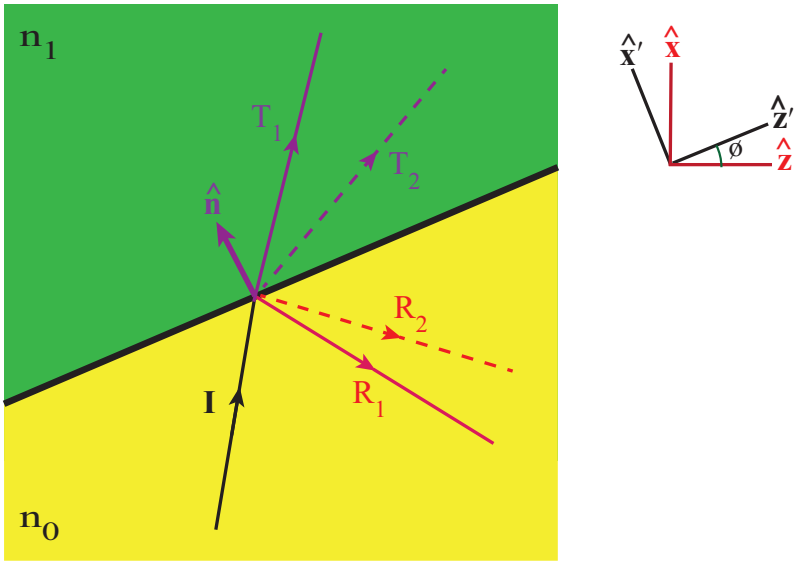


*FIG. 2. Scattering due to a single tangent plane. The electron density has a discontinuous jump across the black line which defines the tangent plane – $\hat{\mathbf{z}}'$ is along the plane while $\hat{\mathbf{x}}'$ is along the normal $\hat{\mathbf{n}}$ to the plane; $\hat{\mathbf{z}}$ is along the ambient magnetic field $\mathbf{B}_0$. The $(\hat{\mathbf{x}}', \hat{\mathbf{z}}')$ plane is a rotation about the $y$ axis through an angle $\phi$ of the $(\hat{\mathbf{x}}, \hat{\mathbf{z}})$ plane. We have assumed that the plasma is homogeneous in the $y$ direction. The ray path of an incident wave is denoted by $I$, while the two reflected waves are $R_1$ and $R_2$, and the two transmitted waves are $T_1$ and $T_2$.*

### 3.1. Boundary Conditions

When evaluating the reflected and transmitted waves, we need to impose boundary conditions at the interface which are consistent with Maxwell equations. We will assume that there are no free charges and currents, and that the incident plane wave is $\mathbf{E}_I = \mathbf{E}_0 e^{ik_{\perp 0}x + ik_{\parallel_0} z}$, where $\mathbf{E}_0$ is a constant amplitude, and $k_{\perp 0}$ is one particular root of (6) for a given $k_{\parallel 0}$. The two reflected and two transmitted plane waves are, respectively,

$$\mathbf{E}_{R1} = \mathbf{E}_{r1} e^{ik_{\perp r1}x + ik_{\parallel r1}z}, \qquad \mathbf{E}_{R2} = \mathbf{E}_{r2} e^{ik_{\perp r2}x + ik_{\parallel r2}z}, \tag{10}$$

$$\mathbf{E}_{T1} = \mathbf{E}_{t1} e^{ik_{\perp t1}x + ik_{\parallel t1}z}, \qquad \mathbf{E}_{T2} = \mathbf{E}_{t2} e^{ik_{\perp t2}x + ik_{\parallel t2}z}, \tag{11}$$

where $\mathbf{E}_{r1}$, $\mathbf{E}_{r2}$, $\mathbf{E}_{t1}$, and $\mathbf{E}_{t2}$ are constant amplitudes. The association of each phase with the corresponding wave is evident from the notation. Imposing Maxwell boundary conditions has two aspects to it. The first aspect is that the phases of all the waves have to be the same along the interface. For $\theta = 0$, (8) connects the $(\hat{\mathbf{x}}, \hat{\mathbf{z}})$ coordinate system to $(\hat{\mathbf{x}}', \hat{\mathbf{z}}')$ coordinate system,

$$\hat{\mathbf{x}} = \cos\phi\, \hat{\mathbf{x}}' + \sin\phi\, \hat{\mathbf{z}}', \qquad \hat{\mathbf{z}} = -\sin\phi\, \hat{\mathbf{x}}' + \cos\phi\, \hat{\mathbf{z}}'. \tag{12}$$

Without loss of generality, we can assume that the interface is along $x' = 0$. The matching of all phases at $x' = 0$ gives,

$$k_{\perp r1}\sin\phi + k_{\parallel r1}\cos\phi = k_{\perp 0}\sin\phi + k_{\parallel 0}\cos\phi, \qquad k_{\perp r2}\sin\phi + k_{\parallel r2}\cos\phi = k_{\perp 0}\sin\phi + k_{\parallel 0}\cos\phi, \tag{13}$$

$$k_{\perp t1}\sin\phi + k_{\parallel t1}\cos\phi = k_{\perp 0}\sin\phi + k_{\parallel 0}\cos\phi, \qquad k_{\perp t2}\sin\phi + k_{\parallel t2}\cos\phi = k_{\perp 0}\sin\phi + k_{\parallel 0}\cos\phi. \tag{14}$$

Since for each wave, $k_\perp$ is related to the corresponding $k_\parallel$ through the dispersion relation (6), (13) and (14) uniquely determine the wave vectors of the reflected and transmitted waves in terms of the wave vector of the

incident wave. The second aspect of Maxwell boundary conditions at the interface has to do with the amplitudes. From Faraday and Ampere-Maxwell equations, the four boundary conditions are the continuity of $\hat{\mathbf{n}} \times \mathbf{B}$ and of $\hat{\mathbf{n}} \times \mathbf{E}$ across $x' = 0$. From Faraday law, $\mathbf{B} = \mathbf{k} \times \mathbf{E}/\omega$. Thus,

$$\Big[\hat{\mathbf{n}} \times (\mathbf{E}_0 + \mathbf{E}_{r1} + \mathbf{E}_{r2})\Big]_{x'=0} = \Big[\hat{\mathbf{n}} \times (\mathbf{E}_{t1} + \mathbf{E}_{t2})\Big]_{x'=0}, \tag{15}$$

$$\Big[\hat{\mathbf{n}} \times (\mathbf{k}_0 \times \mathbf{E}_0 + \mathbf{k}_{r1} \times \mathbf{E}_{r1} + \mathbf{k}_{r2} \times \mathbf{E}_{r2})\Big]_{x'=0} = \Big[\hat{\mathbf{n}} \times (\mathbf{k}_{t1} \times \mathbf{E}_{t1} + \mathbf{k}_{t2} \times \mathbf{E}_{t2})\Big]_{x'=0}, \tag{16}$$

where all the $\mathbf{k}$'s have the form $\mathbf{k} = k_\perp \hat{\mathbf{x}} + k_\parallel \hat{\mathbf{z}}$. It is straightforward to show that the boundary conditions imposed by the two Gauss' laws,

$$\hat{\mathbf{n}} \cdot \Big[\overline{\mathbb{K}}_0 \cdot (\mathbf{E}_0 + \mathbf{E}_{r1} + \mathbf{E}_{r2})\Big]_{x'=0} = \hat{\mathbf{n}} \cdot \Big[\overline{\mathbb{K}}_1 \cdot (\mathbf{E}_{t1} + \mathbf{E}_{t2})\Big]_{x'=0}, \tag{17}$$

$$\hat{\mathbf{n}} \cdot \Big[\mathbf{k}_0 \times \mathbf{E}_0 + \mathbf{k}_{r1} \times \mathbf{E}_{r1} + \mathbf{k}_{r2} \times \mathbf{E}_{r2}\Big]_{x'=0} = \hat{\mathbf{n}} \cdot \Big[\mathbf{k}_{t1} \times \mathbf{E}_{t1} + \mathbf{k}_{t2} \times \mathbf{E}_{t2}\Big]_{x'=0}, \tag{18}$$

are satisfied by the four conditions in (15) and (16). In (18), $\overline{\mathbb{K}}_0$ and $\overline{\mathbb{K}}_1$ are the permittivity tensors for electron densities $n_0$ and $n_1$, respectively.

### 3.2. Poynting Vector and Wave Momentum

The time-averaged Poynting flux for a plane wave is,

$$\langle \mathbf{S} \rangle = \frac{1}{2\mu_0} \mathrm{Re}\,(\mathbf{E} \times \mathbf{B}) = \frac{1}{2\mu_0 \omega} \mathrm{Re}\big[\mathbf{E} \times (\mathbf{k} \times \mathbf{E})\big]. \tag{19}$$

The time-averaged momentum flux is defined as,

$$\langle \boldsymbol{\mathcal{P}} \rangle = \frac{\langle \mathbf{S} \rangle}{v}, \tag{20}$$

where $v = \omega/|\mathbf{k}|$ is the phase speed of the wave.

### 3.3. Energy Conservation and Momentum Conservation

The reflection and transmission coefficients corresponding to the two reflected and two transmitted waves are,

$$R_1 = \left|\frac{\langle \mathbf{S}_{r1} \rangle \cdot \hat{\mathbf{n}}}{\langle \mathbf{S}_I \rangle \cdot \hat{\mathbf{n}}}\right|, \quad R_2 = \left|\frac{\langle \mathbf{S}_{r2} \rangle \cdot \hat{\mathbf{n}}}{\langle \mathbf{S}_I \rangle \cdot \hat{\mathbf{n}}}\right|, \quad T_1 = \left|\frac{\langle \mathbf{S}_{t1} \rangle \cdot \hat{\mathbf{n}}}{\langle \mathbf{S}_I \rangle \cdot \hat{\mathbf{n}}}\right|, \quad T_2 = \left|\frac{\langle \mathbf{S}_{t2} \rangle \cdot \hat{\mathbf{n}}}{\langle \mathbf{S}_I \rangle \cdot \hat{\mathbf{n}}}\right|, \tag{21}$$

where the association of a subscript with the appropriate wave is clear. It can be shown that $R_1 + R_2 + T_1 + T_2 = 1$, which is a statement on the conservation of energy. However, the momentum flux is not conserved,

$$\hat{\mathbf{n}} \cdot \big[\langle \boldsymbol{\mathcal{P}}_{r1} \rangle + \langle \boldsymbol{\mathcal{P}}_{r2} \rangle + \langle \boldsymbol{\mathcal{P}}_{t1} \rangle + \langle \boldsymbol{\mathcal{P}}_{t2} \rangle\big] \neq \langle \boldsymbol{\mathcal{P}}_I \rangle\,. \tag{22}$$

The difference between the right side and the left side of (22) is the momentum imparted to the interface separating $n_0$ from $n_1$. We find that the radiation pressure of the extraordinary or ordinary waves in the electron cyclotron range of frequencies is such that the interface is pushed towards the higher density region [16]. This agrees with Poynting's observations – in plasmas, the higher density region has a smaller permittivity (index of refraction) than a lower density region. Consequently, if an electron cyclotron wave is launched from the low density region, its radiation pressure will tend to push the electron density such that it peaks in the core of the plasma.

## 4. RADIATION PRESSURE ON A CYLINDRICAL FILAMENT

We will model the filamentary structures observed In the scrape-off layer and edge plasma as a cylindrical plasma embedded in a background plasma. The plasma inside and outside the filament is homogeneous and cold; the ratio of the electron densities in the two regions being completely arbitrary. For the Kirchhoff approach to scattering off density turbulence, we could use the Cartesian geometry to derive properties of the reflected and transmitted waves. For a filament, we have to solve the Faraday-Ampere-Maxwell equation in cylindrical coordinates [3] and impose boundary conditions on the surface of the filament. In the planar system, the reflected and transmitted waves were delineated by a two-dimensional plane. For a filament, the reflected and transmitted waves surround the filament; while inside the filament, the electromagnetic fields have a radial structure reminiscent of bounded eigenmodes. The fields outside the filament are referred to as scattered fields while those inside are referred to as filamentary fields. The geometry associated with a filament is shown in Fig. 3. In contrast to planar scattering, filamentary scattering includes effects like diffraction and shadowing.

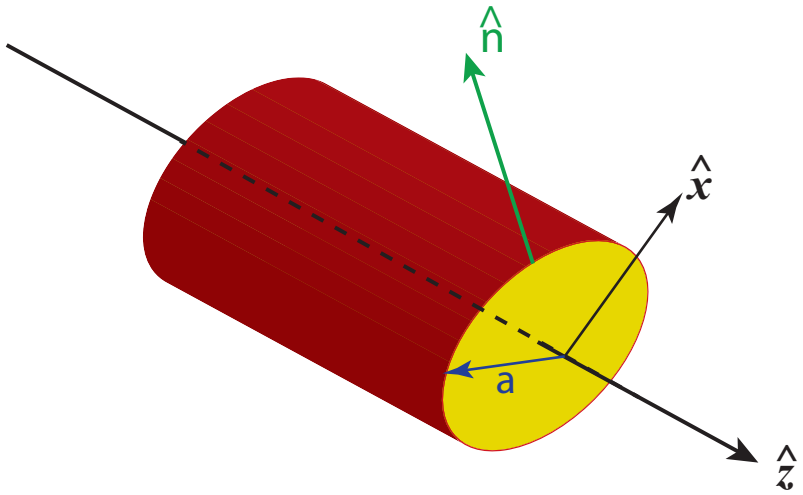


*FIG. 3. The filament is assumed to be a cylindrical plasma of radius a surrounded by a background plasma. The axis of the filament is aligned along the magnetic field $\mathbf{B}_0$, and the electron density inside and outside the filament is assumed to be different. The boundary conditions, imposed on the surface of the filament, are the continuity of the tangential electric and magnetic fields of the waves. The normal to the surface $\hat{\mathbf{n}}$ is along the radial direction with respect to the axis of the filament.*

### 4.1. Maxwell Stress Tensor and Radiation Pressure

From Maxwell equations, the stress tensor is [13],

$$\overline{\mathbb{T}} = \mathbf{E}_R\mathbf{D}_R + \mathbf{H}_R\mathbf{B}_R - \frac{1}{2}\left(\mathbf{E}_R\cdot\mathbf{D}_R + \mathbf{H}_R\cdot\mathbf{B}_R\right)\bar{\mathbb{I}}, \tag{23}$$

where $\mathbf{D} = \epsilon_0\overline{\mathbb{K}}\cdot\mathbf{E}$ is the electric displacement field, and $\mathbf{H}$ is the magnetic intensity with $\mathbf{B} = \mu_0\mathbf{H}$. In (23), the subscript $R$ indicates the real part of the associated fields which are all assumed to be complex. The average over one period $2\pi/\omega$ of the wave yields,

$$\left\langle\overline{\mathbb{T}}\right\rangle = \frac{1}{2}\mathrm{Re}\Big[\epsilon_0\,\mathbf{E}\overline{\mathbb{K}}^*\cdot\mathbf{E}^* + \mu_0\mathbf{H}\mathbf{H}^* - \frac{1}{2}\big(\epsilon_0\,\mathbf{E}\cdot\overline{\mathbb{K}}^*\cdot\mathbf{E}^* + \mu_0\left|\mathbf{H}\right|^2\big)\bar{\mathbb{I}}\Big], \tag{24}$$

where $^*$ indicates the complex conjugate of the associated vector or tensor. The radiation force on a filament is,

$$\boldsymbol{\mathcal{F}} = \int\left\langle\overline{\mathbb{T}}\right\rangle\cdot d\mathbf{A}, \tag{25}$$

where $d\mathbf{A}$ is an area element on the surface of the filament. In the cylindrical coordinate system, $d\mathbf{A} = a\,d\phi\,dz\,\hat{\mathbf{n}}$ where $\phi$ is the azimuthal angle. The force per unit axial length of the filament is,

$$\boldsymbol{\mathcal{F}} = \frac{1}{L}\int_0^L dz\int_0^{2\pi} d\phi\,\left\langle\overline{\mathbb{T}}\left(\rho = a\right)\right\rangle\cdot\hat{\boldsymbol{\rho}}, \tag{26}$$

where $L$ is the axial length of the filament, $\rho$ is the radial coordinate ($\hat{\boldsymbol{\rho}} = \hat{\mathbf{n}}$), and the stress tensor is evaluated on the surface of the filament. Moreover,

$$\left\langle\overline{\mathbb{T}}\left(\rho = a\right)\right\rangle\cdot\hat{\boldsymbol{\rho}} = \left\langle\overline{\mathbb{T}}\left(\rho = a\right)\right\rangle_b\cdot\hat{\boldsymbol{\rho}} - \left\langle\overline{\mathbb{T}}\left(\rho = a\right)\right\rangle_f\cdot\hat{\boldsymbol{\rho}}, \tag{27}$$

where the subscript $b$ indicates that the stress tensor on the surface is determined by the background fields, i.e., the fields just outside the filament, while the subscript $f$ indicates evaluation of the tensor for the filamentary fields. Making use of the boundary conditions, we find that,

$$\begin{aligned}\hat{\boldsymbol{\rho}}\cdot\left\langle\overline{\mathbb{T}}\left(\rho = a\right)\right\rangle\cdot\hat{\boldsymbol{\rho}} &= \frac{\epsilon_0}{4}\Big[K_{b\perp}\left|E_{I\rho} + E_{b\rho}\right|^2 - K_{f\perp}\left|E_{f\rho}\right|^2 + \\ &\qquad \left(K_{f\perp} - K_{b\perp}\right)\left|E_{f\phi}\right|^2 + \left(K_{f\parallel} - K_{b\parallel}\right)\left|E_{fz}\right|^2\Big]_{\rho=a}, \qquad (28)\\ \hat{\boldsymbol{\phi}}\cdot\left\langle\overline{\mathbb{T}}\left(\rho = a\right)\right\rangle\cdot\hat{\boldsymbol{\rho}} &= 0, \qquad (29)\\ \hat{\mathbf{z}}\cdot\left\langle\overline{\mathbb{T}}\left(\rho = a\right)\right\rangle\cdot\hat{\boldsymbol{\rho}} &= 0, \qquad (30)\end{aligned}$$

where the subscripts $f$ and $b$ correspond to the filament plasma and the background plasma, respectively, and the subscript $I$ is for the incident wave. In the cylindrical coordinate system, the fields are expressed as $\mathbf{E} = E_\rho\,\hat{\boldsymbol{\rho}} + E_\phi\,\hat{\boldsymbol{\phi}} + E_z\,\hat{\mathbf{z}}$. From the results in (28)–(30) it is evident that the radiation force due to RF waves is in the radial direction and depends on the azimuthal angle only; the variation along $z$ being of the form $\exp(ik_z z)$. The RF waves do not induce any shear force on the filament. In the example shown in Fig. 4, we note that the radial force is not uniform azimuthally. Consequently, the radiation force leads to radial displacement and azimuthal distortion.

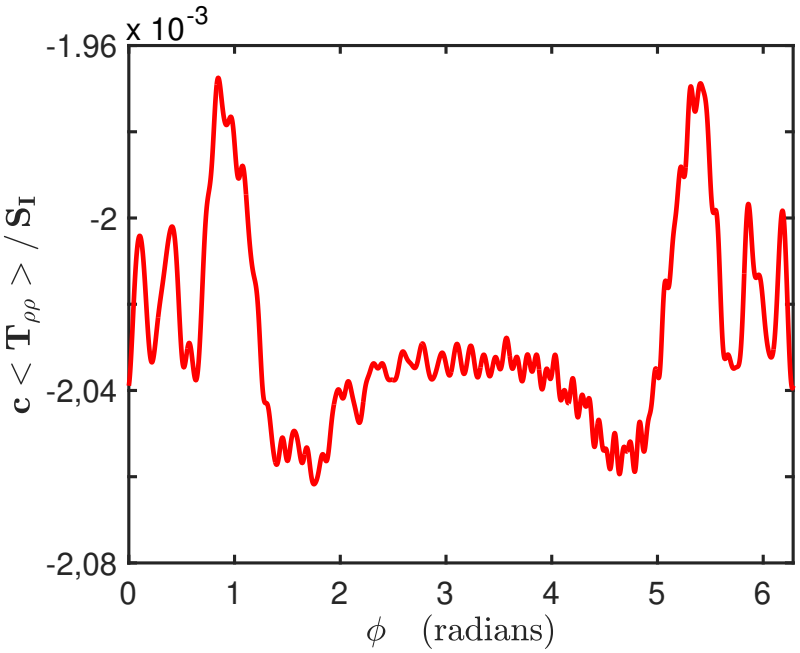


*FIG. 4. The radial component of radiation force* $\hat{\boldsymbol{\rho}} \cdot \left\langle \overline{\mathbb{T}}\,(\rho = a) \right\rangle \cdot \hat{\boldsymbol{\rho}}$*, from (28), normalized to the Poynting flux of the incident wave as a function of the azimuthal angle* $\phi$*. The physics unit associated with the ordinate is* $(nN/m)/(W/m^2)$*. The incident wave is an ordinary wave in the electron cyclotron range of frequencies.The parameters used for this plot are: wave frequency* $\omega/2\pi = 170$ *GHz,* $B_0 = 5$ *T,* $a = 1$ *cm, background electron density* $= 5 \times 10^{18}$ $m^{-3}$*, electron density inside the filament* $= 6.5 \times 10^{18}$ $m^{-3}$*, and* $ck_\parallel/\omega = 0.2$ *for the incident wave.*

From (26) and (28), the radial component of the radiation force per unit axial length of the filament is,

$$\mathcal{F}_\rho = a \int_0^{2\pi} d\phi\, \hat{\boldsymbol{\rho}} \cdot \left\langle \overline{\mathbb{T}}\,(\rho = a) \right\rangle \cdot \hat{\boldsymbol{\rho}}. \tag{31}$$

The power flux of the incident wave is,

$$S_I = |\langle \mathbf{S}_I \rangle| = \frac{1}{2} \sqrt{\frac{\epsilon_0}{\mu_0}}\, |\mathbf{E}_0|^2\,, \tag{32}$$

where $\mathbf{E}_0$ is the electric field amplitude of the incident wave. The ratio $\mathcal{F}_\rho/S_I$ is plotted in Fig. 4.

## 5. CONCLUSIONS

The radiation pressure of RF waves on turbulence is a significant effect that can be observed experimentally. We have discussed two different formulations of the radiation pressure. The first model is applicable to planar fluctuations where we can use the Kirchhoff tangent plane approximation. The radiation pressure follows Poynting's observations and is such that higher densities are pushed away from the antenna and towards the core of a plasma. The second model deals with filaments that are present in the scrape-off layer. The filaments are approximated as cylindrical plasmas aligned along the magnetic field. The radiation pressure is evaluated using the Maxwell stress tensor. We find that the radiation pressure leads to a radial displacement of the filament and to its azimuthal distortion. There are no shear forces on the surface of a filament.

**ACKNOWLEDGEMENTS**

AKR is supported by Department of Energy Grants DE-FG02-91ER-54109 and DE-SC0018090.

**REFERENCES**

[1] GRULKE, O., TERRY, J. L., LaBOMBARD, B., ZWEBEN, S. J., Radially propagating fluctuation structures in the scrape-off layer of Alcator C-Mod, Phys. Plasmas, 13 (2006) 012306-1–012306-7.

[2] RAM, A.K., HIZANIDIS, K., KOMINIS, Y., Scattering of radio frequency waves by blobs in tokamak plasmas, Phys. Plasmas, 20 (2013) 056110-1–056110-10.

[3] RAM, A.K., HIZANIDIS, K., Scattering of radio frequency waves by cylindrical density filaments in tokamak plasmas, Phys. Plasmas, 23 (2016) 022504-1–022504-17.

[4] KÖHN, A., HOLZHAUER, E., LEDDY, J., THOMAS, M. B., VANN, R. G. L., Influence of plasma turbulence on microwave propagation, Plasma Phys. Control. Fusion, 58 (2016) 105008-1–105008-9.

[5] Z. IOANNIDIS, Z., RAM, A.K., HIZANIDIS, K., TIGELIS, I.G., Computational studies on scattering of radio frequency waves by density filaments in fusion plasmas, Phys. Plasmas 24 (2017) 102115-1–102115-13.

[6] VALVIS, S. I., RAM, A. K., HIZANIDIS, K., PAPAGIANNIS, P., PAPADOPOULOS, A., ZISIS, A., TIGELIS, I. G., GLYTSIS, E., Scattering of radio frequency waves by cylindrical filaments with general orientation relative to the magnetic field, J. Plasma Phys., 84 (2018) 745840604-1– 745840604-28.

[7] SNICKER, A., POLI, E., MAJ, O., GUIDI, L., KÖHN, A., WEBER, H., CONWAY, G., HENDERSON, M., SAIBENE G., The effect of density fluctuations on electron cyclotron beam broadening and implications for ITER, Nuclear Fusion, 58 (2018) 016002-1–016002-13.

[8] VALVIS, S. I., RAM, A. K., HIZANIDIS, K., Interaction of radio frequency waves with cylindrical density filaments: scattering and radiation pressure, J. Plasma Phys., 87 (2021) 905870612-1–905870612-37.

[9] McDERMOTT, R. M., ANGIONI, C., CAVEDON, M., KAPPATOU, A., DUX, R., FISCHER, R., MANAS, P., Validation of low-Z impurity transport theory using boron perturbation experiments at ASDEX upgrade, Nuclear Fusion, 62 (2021) 026006-1–026006-21.

[10] POYNTING, J. H., Radiation pressure, The London, Edinburgh, and Dublin Philosophical Magazine and Journal of Science, 9 (1905) 393–406.

[11] BECKMANN, P., SPIZZICHINO, A., The Scattering of Electromagnetic Waves from Rough Surfaces, Artech House, Boston (1987).

[12] OGILVY, J. A., Theory of Wave Scattering from Random Rough Surfaces, Institute of Physics Publishing, Philadelphia (1991).

[13] STRATTON, J. A., Electromagnetic Theory, McGraw-Hill, New York (1941).

[14] GRIFFITHS, D. J., Introduction to Electrodynamics, Cambridge University Press, Cambridge (2017).

[15] BERS, A., Plasma Physics and Fusion Plasma Electrodynamics, Volume 1, Oxford University Press, New York (2016).

[16] RAM, A. K., HIZANIDIS, K., Radiation pressure by electron cyclotron waves on density fluctuations, EPJ Web of Conferences, 227 (2023) 01001-1–01001-8.